



Different 2D and 3D mask constraints synthesis for large array pattern shaping

Ahmed Jameel Abdulqader

College of Electronics Engineering, Ninevah University, Mosul, Iraq

Research Paper

Cite this article: Abdulqader AJ (2023). Different 2D and 3D mask constraints synthesis for large array pattern shaping. *International Journal of Microwave and Wireless Technologies* 1–9. <https://doi.org/10.1017/S1759078723001198>

Received: 02 June 2023
Revised: 28 September 2023
Accepted: 03 October 2023

Keywords:

array factor; beam pattern shaping; contour pattern; large array; mask constraint; multi-beam; PSO algorithm; pencil beam; sidelobes; wide flat beam

Email: ahmed.abdulqader@uoninevah.edu.iq

Abstract

In this article, different 2D and 3D mask styles for synthesizing large array pattern shaping to meet the requirements of modern applications are realized. The composition of the different beam pattern shaping is achieved by comparing the array factor with the proposed masks whose details (upper and lower borders) are predefined according to the designer. The generated pattern shapes are as follows: unscanned 2D single-pencil beam, scanned 2D pencil beam, 2D multi-beam scanning, 2D wide flat beam with little ripple, unscanned 3D single-pencil beam, 3D multi-beam scanning, and footprint (or contour) pattern for linear and planar arrays. The process of constructing these patterns is followed by predicting the amplitude-only weights (i.e., the phase weighting is considered zero in all computations) of the elements using the particle swarm optimization algorithm. In all proposed masks, different sidelobe levels are controlled, ranging from -20 to -100 dB. Also, the radiated beamwidth is controlled, ranging from 0.1334 rad (7.6 deg.) to 0.4 rad (23 deg.). The analysis and construction of linear and planar array arrangements depend on the formulation of antenna array theory through the implementation of the proposed (estimated) equations using MATLAB code. The simulation results showed the effectiveness of the proposed methods in controlling the pattern shape according to the required modern trends.

Introduction

Optimal tuning of large antenna arrays is an important parameter in modern communication applications such as MIMO in the fifth generation [1], radar [2], satellite [3], and many other scenario applications. Some of these applications require a configurable beam pattern such as a narrow directive beam of the radiated power to meet the required coverage requirements. Shaping of a beam pattern reduces the wastage of transmitter energy and avoids unwanted radiations that are directed to the coverage site [4]. Among the various methods for achieving this property, the ones that involve the best utilization of the available degrees of freedom (i.e., the most efficient use of the antenna array resources) are those that aim to mask-shaped covering constraints for beam pattern synthesis.

Some of the above applications require synthesizing beam steering with high directivity concentration, and it is also possible to generate several beams with different shapes from the same aperture [5]. Where several beams can be generated through several methods, including the use of the multi-feed reflector [6], switched beam technique [7], or array beam design depending on lenses [8]. In addition, it is possible to improve the shaped beam as a contour that matches the shape of the area to be covered. Contour patterns can be built either through a shaped parabolic reflector [9], projection matrix method [10], or based on the weights of the elements in the beamforming network [11].

In the case of determining the structure of the antenna array, while the feeding elements are the only unknowns in building the desired shaped beam pattern, then the problem is solved depending on global optimization methods, whether in sum or difference patterns. In fact, without imposing any restrictions on the array factor in terms of excitation distribution or array shape, the problem is depicted as a convex problem that can be improved either by using convex algorithms or evolutionary algorithms. By doing so, the optimal compromise can be successfully addressed by optimizing patterns based on amplitude only, phase only, or both for single-pulse radar communications [12, 13].

Regrettably, there are various situations imposed on the installation of patterns of a certain format which remains an unresolved normative problem [14]. Indeed, regardless of methods that do not employ all available degrees of freedom (i.e., those that seek to generate a single null or a set of nulls or are unable to significantly reduce sidelobes [12]), the problem has been solved by global optimization methods only in the case that it maintains directivity in the beam pattern.

Currently, the formation of radiation beams with multiple requirements occupies the minds of researchers such as narrow directive beams [15], contour coverage patterns [4], and circular

© The Author(s), 2023. Published by Cambridge University Press in association with the European Microwave Association. This is an Open Access article, distributed under the terms of the Creative Commons Attribution licence (<http://creativecommons.org/licenses/by/4.0>), which permits unrestricted re-use, distribution and reproduction, provided the original article is properly cited.

flat-top patterns [16]. These capabilities have allowed the development of interesting solutions for many other cases [17]. In fact, the problem is usually addressed by resorting to global optimization algorithms or sampling algorithms [18]. Hence, in most cases of optimization, it is expected that the computational complexity using the above algorithms increases dramatically with the number of unknowns, which can prevent the actual access to the global optimization level, especially in the case of large arrays.

Modern curricula partially overcome the above difficulties in the existing curricula [19–24]. The main idea of these approaches is to control the beam pattern by reducing the constraints of forming a pattern mask by either relying on phase-only optimization [12] or building amplitude-only clusters [25]. These techniques yielded good results in norm cases and showed interesting features such as the ability to find several solutions that all correspond to the desired beam pattern formation under the mask constraint.

Several optimizations, analysis, and iterative [26, 27] methods have been proposed to construct the different coverage patterns described above, whether in linear or planar arrays. For example, in paper [28], a method is proposed based on the arrangement of appropriate multiple field distributions on the array aperture but without controlling the level of the sidelobes. In paper [29], the successive iteration method is introduced based on adding a series of corrective patterns. In paper [30], the method of formation of a pattern using Taylor with superposition primitives based on a genetic algorithm (GA) with control of the sidelobe levels (SLLs) has been presented. In papers [12, 13, 20, 25], the researchers proposed a set of methods for installing sub-arrays by controlling some characteristics of the coverage pattern in addition to reducing the complexity of the system from a practical point of view. In addition to many well-known classical methods such as the Fourier transform, Chebyshev polynomials, and Schelkunoff as these methods deal with excitation (amplitude and phase) levels.

Most of the current shaping methods work directly to improve excitation weights. These approaches superimpose phased beam patterns by placing them in specific null locations with optimal energy levels [31]. Optimization by evolutionary algorithms (GA and particle swarm optimization [PSO]) uses peak angle and power to reduce ripples in the region of focused energy (main beam) while reducing sidelobe energies [32]. Also, these algorithms work to determine multiple scanning beams and energy levels for each angle to obtain the final beam shape. This approach is simple and can be easily implemented in linear and planar (square, rectangular, and circular) arrays and manipulates ripples and sidelobes together.

In this article, mathematical analysis and detailed structural construction of a 2D and 3D beam pattern synthesis based on efficient masks shape are formulated. The composition of 2D patterns of linear arrays and arrangements of planar arrays corresponding to 3D patterns is achieved using amplitude-only control. The synthesis of different beam patterns in linear and planar constructs with different radiated beamwidths (RBWs) and varying SLL was investigated. The pattern shapes are as follows: unscanned 2D and 3D single-pencil beam, scanned 2D and 3D pencil beam, 2D and 3D multi-beam scanning, and 2D (flat) and 3D (footprint or contour) beam with little ripple patterns. The PSO algorithm is used to control the amplitude values on the antenna array. The linear and planar array analysis was implemented using MATLAB code through the array factor (AF) in coordination with the proposed mask functions. Computational results prove the efficiency of the proposed methods and structures in building the required patterns in modern applications trends.

Study methodology

The performance of the global optimization method will be presented using a set of tests on linear and planar arrays to form the following required beams that have high practical relevance:

- Formation of a single unscanned 2D and 3D pencil beam pattern for the linear and planar arrays, respectively. These patterns can be used to reduce the power of the transmission system by providing the same field strength for the coverage area in mobile communications (e.g., MIMO in the fifth generation).
- The formation of a single scanned 2D and 3D pencil beam pattern at different directions is determined by the designer with control over the sidelobes at different low levels. This type of pattern must be provided in many cases to achieve the requirements of the transmitting systems or to reduce noise or interference in the receiving systems.
- Forming multiple 2D and 3D beam patterns in different directions to find coverage requirements in the fifth generation and satellite coverage systems, as well as directing several beams to mobile stations within the coverage distance of a cellular base station.
- Forming a 2D flat beam pattern and 3D square footprint. This type of beam can be used to reduce the field strength within the geographical area of the satellite station.

The proposed optimization approach in this study can be depicted as follows. A dimensional array of N elements and a two-dimensional with $N \times M$ elements are used to synthesize the aforementioned patterns with high accuracy. This goal is achieved through the complex excitation (amplitude and phase) of each element individually. The normalization of the element coefficient, whether in the linear or planar array, leads to degrees of freedom of the amount of the total number of elements minus one for the excitation of the feed, which can be referred to as $y \in G$, where $G \in C^{N-1}$ or $G \in C^{N \times M-1}$, which is represented the area of the optimization solution. The target of the optimization, in this case, is to estimate the excitation of the elements to tune the required patterns by reducing the error between the synthesized and desired patterns.

Mathematical formulation and description of optimization method

Let's think about achieving a practical application of the arrays (linear and planar), where certain conditions must be adhered to in terms of illumination (e.g., a footprint pattern on certain coverage cells). In this case, the beam pattern is under the required constraints to fit a specific shape. Through this principle, several forms of the pattern are implemented according to the required application. In this way, a suitable optimization algorithm such as GA or PSO can be proposed to realize these ideas.

To formulate the appropriate mathematical model for this study, first, the linear array factor (LAF) of the uniform linear array, which consists of N isotropic elements, is considered. As well known, the AF is used to calculate the total radiation field of an array aperture. This field is calculated by multiplying the electric field of the single element with the LAF. The LAF consists of several control components to build the required patterns. In this study, the focus is on improving the excitation of each element. A single element in the array radiates an electric field in the form of $\frac{w}{4\pi q} e^{-jkq}$, where w is the complex excitation, k is the wave number and can be calculated

by $2\pi/\lambda$, where λ is the wavelength. Depending on the electric fields of the elements, the total LAF can be written in the form of the sum of the fields, as follows:

$$\begin{aligned} \text{LAF} &= \frac{w_1}{4\pi q_1} e^{-jk\vec{q}_1 \cdot \vec{t}_1} + \frac{w_2}{4\pi q_2} e^{-jk\vec{q}_2 \cdot \vec{t}_2} + \dots + \frac{w_{N-1}}{4\pi q_{N-1}} e^{-jk\vec{q}_{N-1} \cdot \vec{t}_{N-1}} \\ &= \sum_{i=1}^N \frac{w_i}{4\pi q_i} e^{-jk\vec{q}_i \cdot \vec{t}_i} \end{aligned} \tag{1}$$

where q_i is the location vector of the elements within the array, \vec{t}_i is the point vector for each element located in (x, y) in the axes of the array, where

$$\vec{q}_i = x_i \vec{t}_x + y_i \vec{t}_y \tag{2}$$

and

$$\vec{t}_i = \sin \theta \cos \phi \vec{t}_x + \sin \theta \sin \phi \vec{t}_y \tag{3}$$

Then,

$$\text{LAF} = \sum_{i=1}^N \frac{w_i}{4\pi q_i} [e^{-jkx_i u}] \tag{4}$$

where $u = \sin \theta$, θ is the direction of the main beam. Then, the total electromagnetic field can be calculated by

$$LE_t = \text{single element field (SEF)} \times \text{LAF} \tag{5}$$

In the case of the planar array, the planar array factor (PAF) can be written as

$$\begin{aligned} \text{PAF} &= \begin{bmatrix} \frac{w_{1,1}}{4\pi q_{1,1}} e^{-jk\vec{q}_{1,1} \cdot \vec{t}_{1,1}} & \dots & \frac{w_{1,N-1}}{4\pi q_{1,N-1}} e^{-jk\vec{q}_{1,N-1} \cdot \vec{t}_{1,N-1}} \\ \vdots & \ddots & \vdots \\ \frac{w_{M-1,1}}{4\pi q_{M-1,1}} e^{-jk\vec{q}_{M-1,1} \cdot \vec{t}_{M-1,1}} & \dots & \frac{w_{M-1,N-1}}{4\pi q_{M-1,N-1}} e^{-jk\vec{q}_{M-1,N-1} \cdot \vec{t}_{M-1,N-1}} \end{bmatrix} \end{aligned} \tag{6}$$

In this case, \vec{t}_i is the point vector placed at (x, y, z) as

$$q_{ij} = x_{ij} \vec{t}_x + y_{ij} \vec{t}_y + z_{ij} \vec{t}_z \tag{7}$$

where \vec{t} in this case equal to

$$\vec{t}_{ij} = \sin \theta \cos \phi \vec{t}_x + \sin \theta \sin \phi \vec{t}_y + \cos \theta \vec{t}_z \tag{8}$$

Then, PAF can be written as follows:

$$\text{PAF} = \sum_{n=1}^N \sum_{m=1}^M \frac{w_{nm}}{4\pi q_{nm}} [e^{-jkx_{nm}u} e^{-jky_{nm}v} e^{-jkz_{nm}s\sqrt{1-u^2-v^2}}] \tag{9}$$

where u is the azimuth plane equal to $\sin \theta \cos \phi$, v is the elevation plane equal to $\sin \theta \sin \phi$, $s = \cos \theta$, $\theta = \cos^{-1} \sqrt{1-u^2-v^2}$, and $\phi = \tan^{-1} \frac{v}{u}$. Then, the radiation pattern space can be defined by $u^2 + v^2 + s^2 = 1$. The final field can be written as

$$PE_t = \text{SEF} \times \text{PAF} \tag{10}$$

An evolutionary optimization algorithm such as PSO can be used to predict excitation values to find the desired 2D and 3D pattern shapes. In the next section, the PSO algorithm is explained and then applied to this study.

PSO algorithm approach

In paper [33], the researchers carried out the first research study in applying the PSO algorithm to some electromagnetic problems. The algorithm is described in this research as a computational

method based on random search and depends on the movement and intelligence of flocks. In our research, it is appropriate to use the PSO algorithm to estimate the excitation values of the elements to build the required patterns.

In most practical application problems, the process of searching for all possible values of G in the C calculation search is not possible even if the values of M and N are small. On this basis, the PSO algorithm is employed to search for optimal excitation vector (or matrix) values for the elements through a controlled computational model.

The algorithm starts by generating a set of random particles within the desired search range $G_0^i, i \in G \{1, \dots, r\}$, where r is the number of generated random particles. Each particle has an optimal solution called personal best (p_b), as well as a global best (p_g) solution and this solution is the best solution achieved by any particle (individual). The particles aspire to reach the global position by updating their velocities in each iteration through the use of the following equations [21]:

$$v_{k+1}^i = \left\{ w_p v_k^i + \left(c_1 r_1^k (p_{b_k}^i - x_k^i) + c_2 r_2^k (p_{g_k}^- x_k^i) \right) / \Delta t \right\} \tag{11}$$

$$x_{k+1}^i = x_k^i + v_{k+1}^i \cdot \Delta t \tag{12}$$

where v_k^i is the moving velocity of the particle within the search range, x_k^i is the position of the particle, and w_p is the weight of inertia allocated to the particle and is determined within the range [0,1]. $c_1 = c_2$, which are the constants of scaling, through them, how the particle is affected by the global and personal best is determined, and their values are also determined within the range [0,1]. In this research, the values of $c_1 = c_2 = 1.7$ were determined. r_1 and r_2 are continuous random variable numbers of a uniform distribution according to [0,1]. Δt represents the step size during the execution of the algorithm and its value is determined by the designer. The increase in the value of the mean k signifies a new iteration if the criteria are not met to stop the algorithm. The maximum number of iterations can be chosen through the proposed cost function. After initializing the algorithm, a final cost function is added to form the radiated beams, known as a mask (envelope) that is determined at different levels according to the imposed constraints:

$$ML(u)_{\text{lower level mask}} \leq |LAF(u)| \leq MU(u)_{\text{upper level mask}} \tag{13}$$

$$ML(u, v)_{\text{lower surface mask}} \leq |PAF(u)| \leq MU(u, v)_{\text{upper surface mask}} \tag{14}$$

The basis of the PSO algorithm is to reduce the square root value of the component F_x :

$$\begin{aligned} F_x &= \sum_{n_f=1}^{N_f} \left[\left| LAF - MU(u)_{\text{upper level mask}} \right|^2 \right. \\ &\quad \left. + \left| LAF - ML(u)_{\text{lower level mask}} \right|^2 \right]_{\text{for 2D patterns}} \end{aligned} \tag{15}$$

$$\begin{aligned} F_x &= \sum_{n_f=1}^{N_f} \left[\left| PAF - MU(u, v)_{\text{upper surface mask}} \right|^2 \right. \\ &\quad \left. + \left| PAF - ML(u, v)_{\text{lower surface mask}} \right|^2 \right]_{\text{for 3D patterns}} \end{aligned} \tag{16}$$

where N_f is the resolution points.

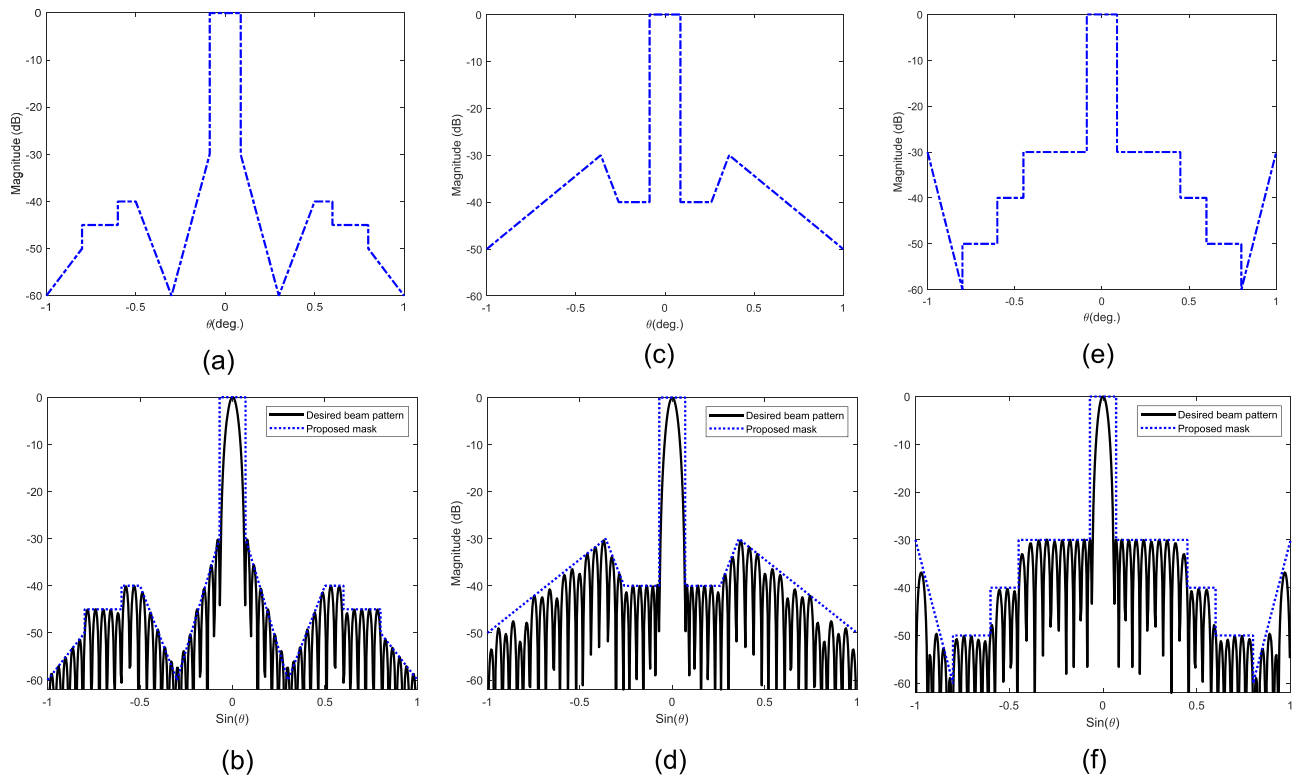


Figure 1. Unscanned single-beam pattern configuration (a, c, and d) the set of desired mask template, (b, d, and f) the set of desired single-beam pattern.

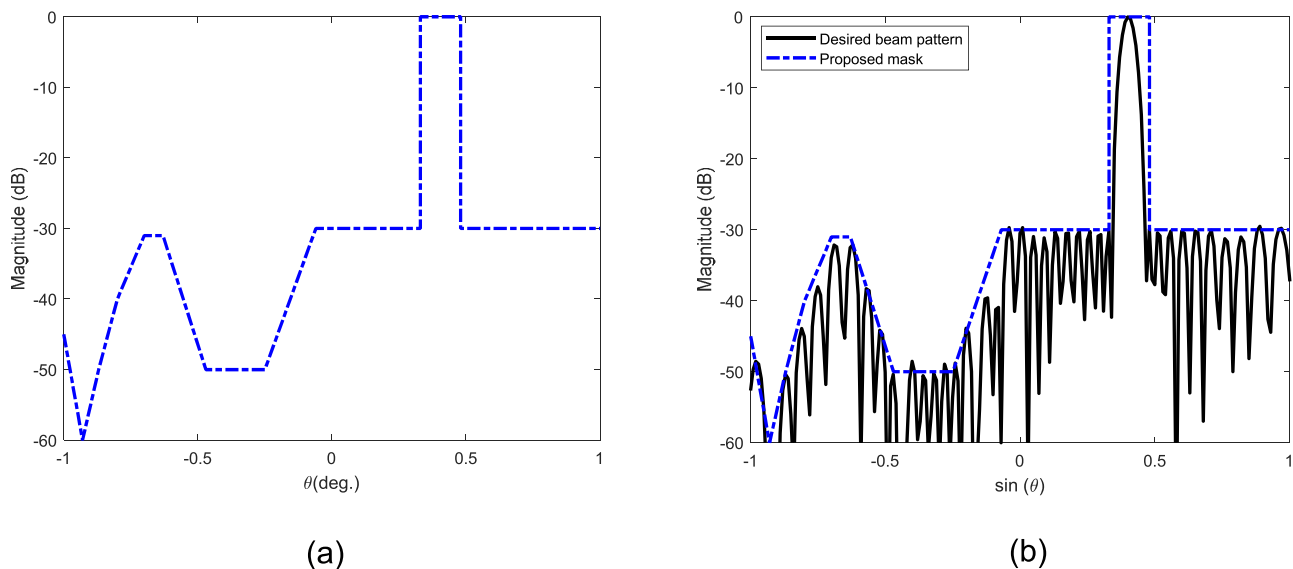


Figure 2. Scanned single-beam pattern configuration (a) the desired mask template, (b) the desired single-beam pattern steered at $\theta = 0.4$ rad.

Simulation results and discussion

In this section, a set of tests are introduced to investigate the effectiveness of the proposed approaches in the generation of different 2D and 3D radiation patterns. In all tests, the PSO algorithm population size of 50 is selected. Also, in all tests, amplitude-only excitation is employed during the implementation of the algorithm. This means that the phase feed is considered zero. The upper and lower limits of the amplitude values are chosen between 0 and 1. As well, the distance between the elements is considered

constant, so it is not taken into account in the optimization process, and its value is 0.5λ .

Linear array pattern shaping (2D Pattern)

Irregular arrays in terms of excitation elements have the ability to provide robust beam pattern characteristics compared to regular arrays through a few physically optimized elements [34]. Assuming any proposed mask requires sufficient degrees of freedom to generate the desired pattern, this is provided by irregular arrays.

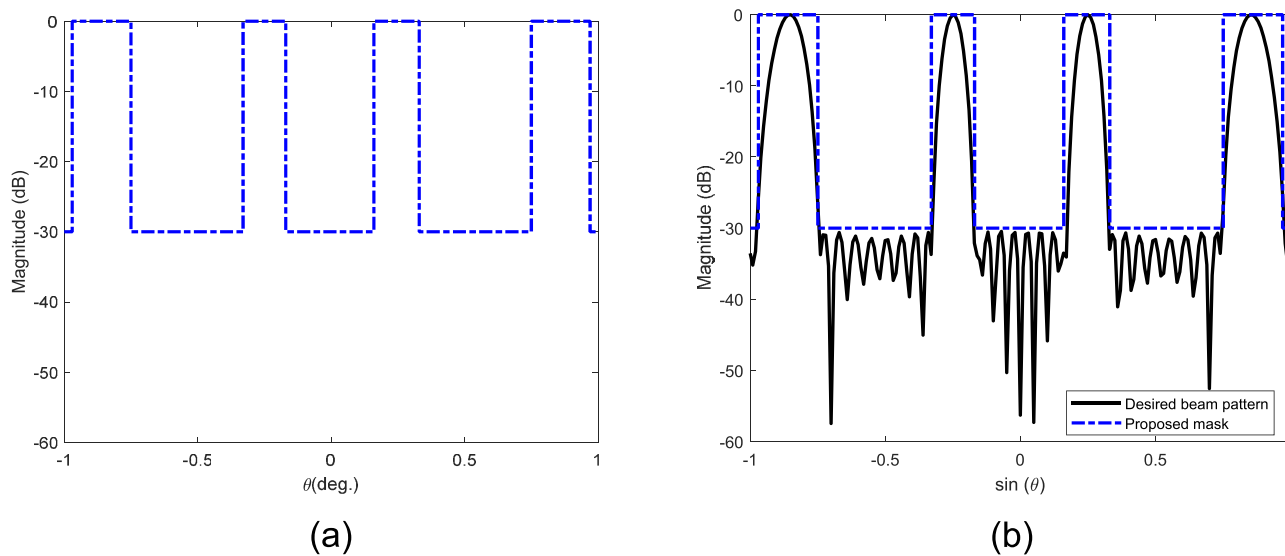


Figure 3. Four-beams pattern configuration: (a) the desired mask template, (b) the desired multi-beam pattern steered at different directions.

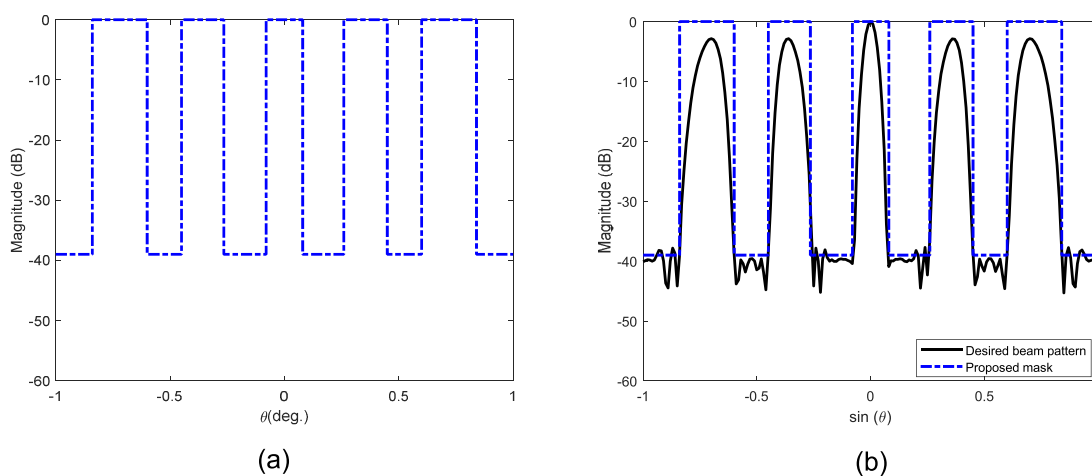


Figure 4. Five-beams pattern configuration: (a) the desired mask template, (b) the desired multi-beam pattern steered at different directions.

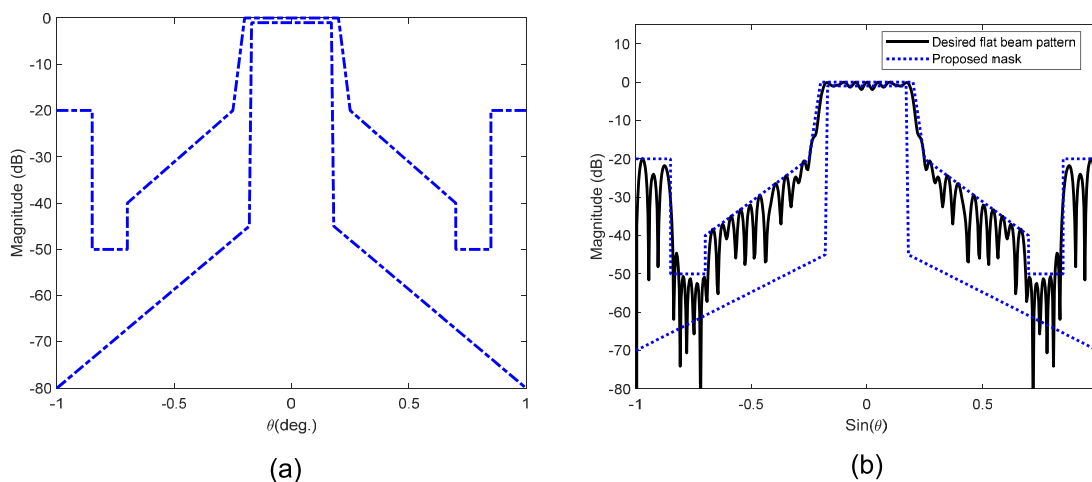


Figure 5. Wide flat beam pattern configuration: (a) the desired mask template, (b) the desired wide flat pattern.

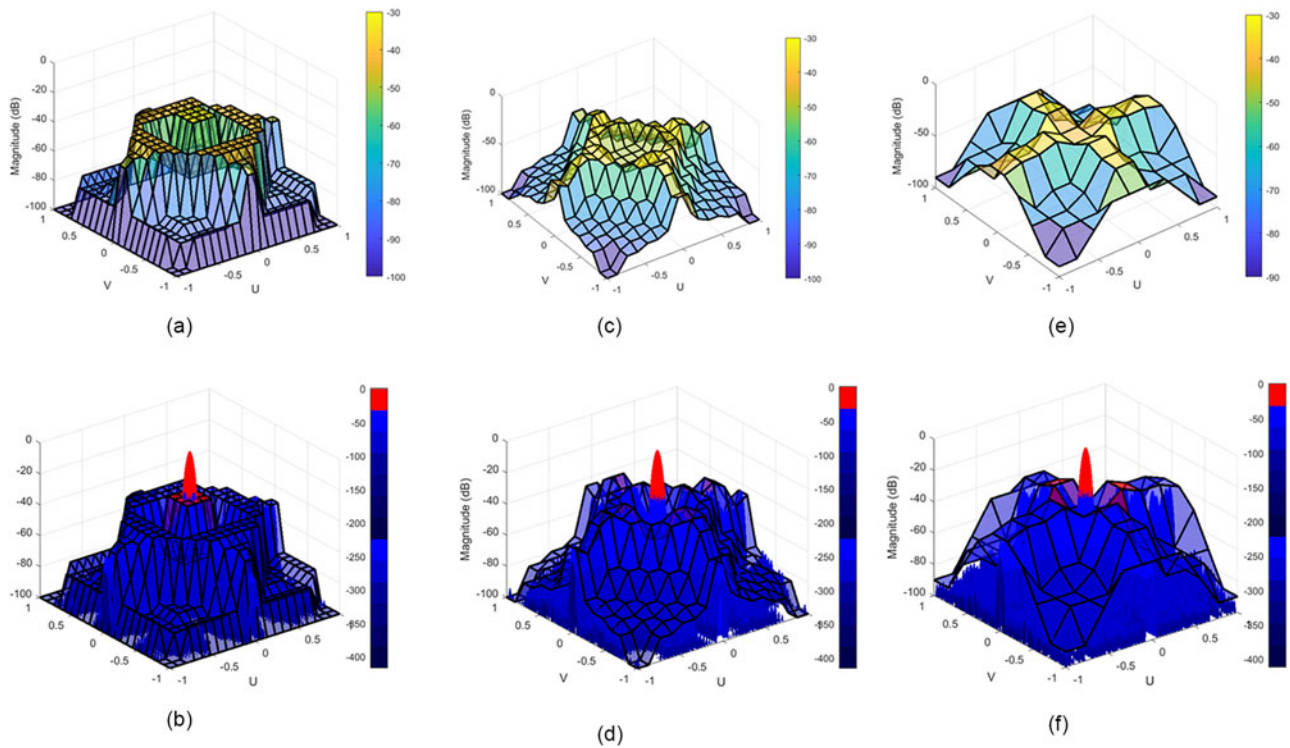


Figure 6. Unscanned 3D single-pencil beam pattern configuration: (a, c, and d) a set of desired 3D mask grid template, (b, d and f) a set of desired 3D single-pencil beam pattern.

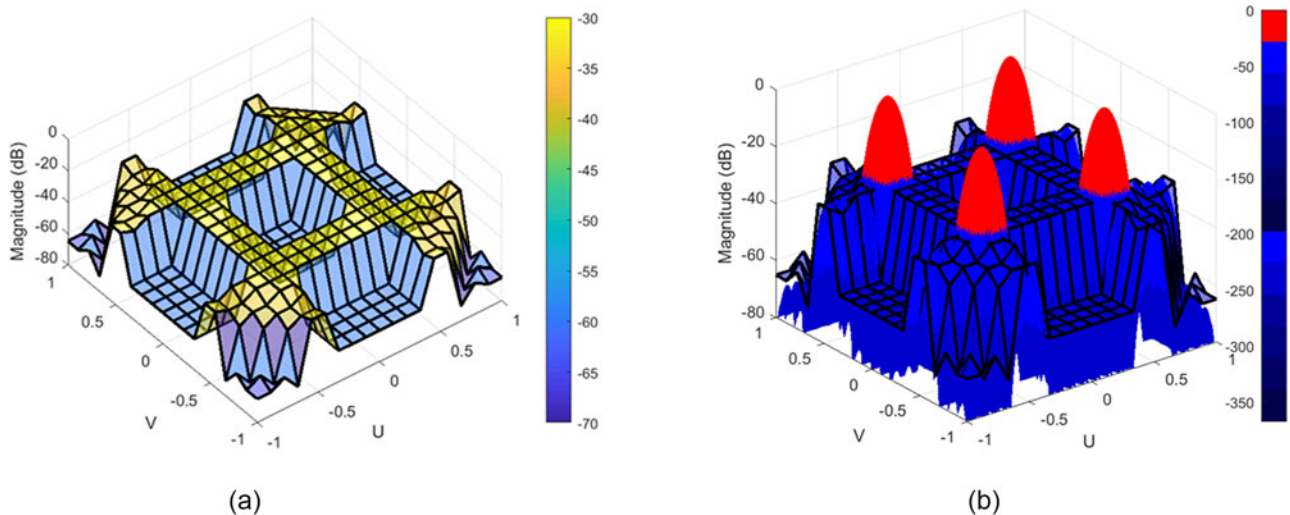


Figure 7. Scanned 3D four-beams pattern configuration: (a) a desired 3D mask grid template, (b) a desired 3D four-beam pattern.

Test1 (Linear array): for the first test, an unscanned irregular amplitude-only linear array composed of $N = 50$ is examined. Figure 1 shows a set of single electric field patterns with suggested masks for the pencil beam at $\theta = 0$ achieved using the PSO algorithm. In this case, 2D masks with different levels of sidelobes $-60 \leq \text{SLL (dB)} \leq -30$ and RBW of 0.1334 rad (7.6 deg.) are prepared.

It is observed through these figures that a pattern can be built compatible with the proposed masks without exceeding the borders of the mask patch. These masks are suggested based on the concentration of energy in the main beam, with the cancellation

or nullification of the interference that the system may be exposed to due to noise sources. The PSO algorithm determines the amplitude excitation value for each element so that the pattern contains a main beam in direction of $\theta = 0$, and nulls or reduced sidelobes in the other directions. In this way, the pattern is ready and suitable to be used in the desired application.

Test 2 (Linear array): for the second test, a scanned irregular amplitude-only linear array composed of $N = 50$, a beam steering at $\theta = 0.4$ rad (23 deg.) is examined. Figure 2 shows the generation of a 2D single electromagnetic pencil beam pattern according to the proposed 2D mask. It can be seen from this figure that the width of

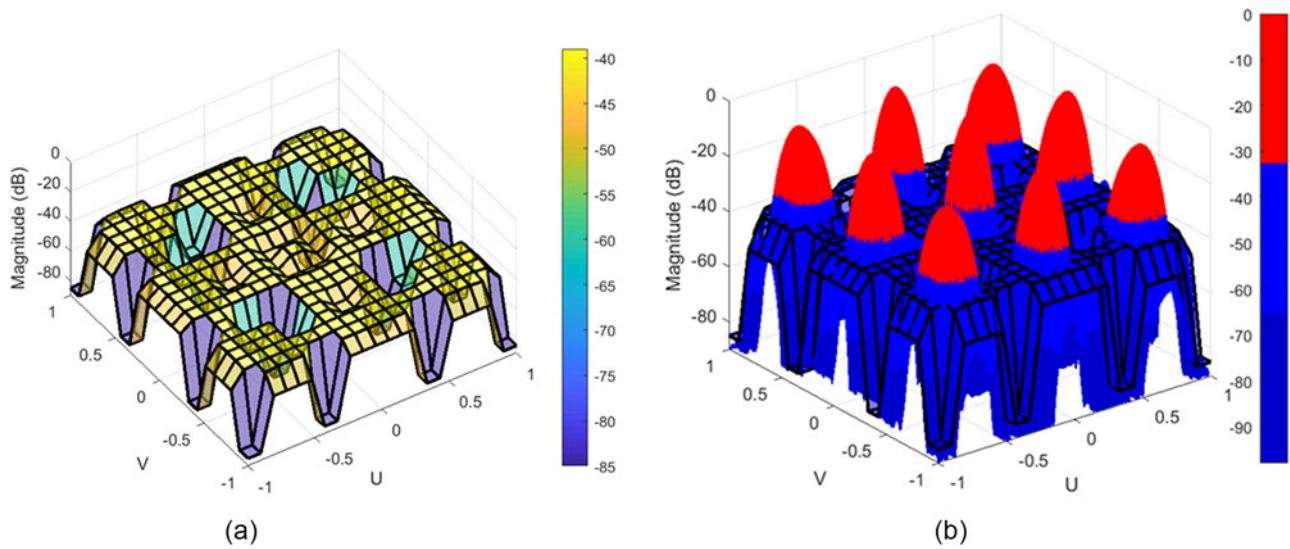


Figure 8. Scanned 3D nine-beams pattern configuration: (a) a desired 3D mask grid template, (b) a desired 3D nine-beam pattern.

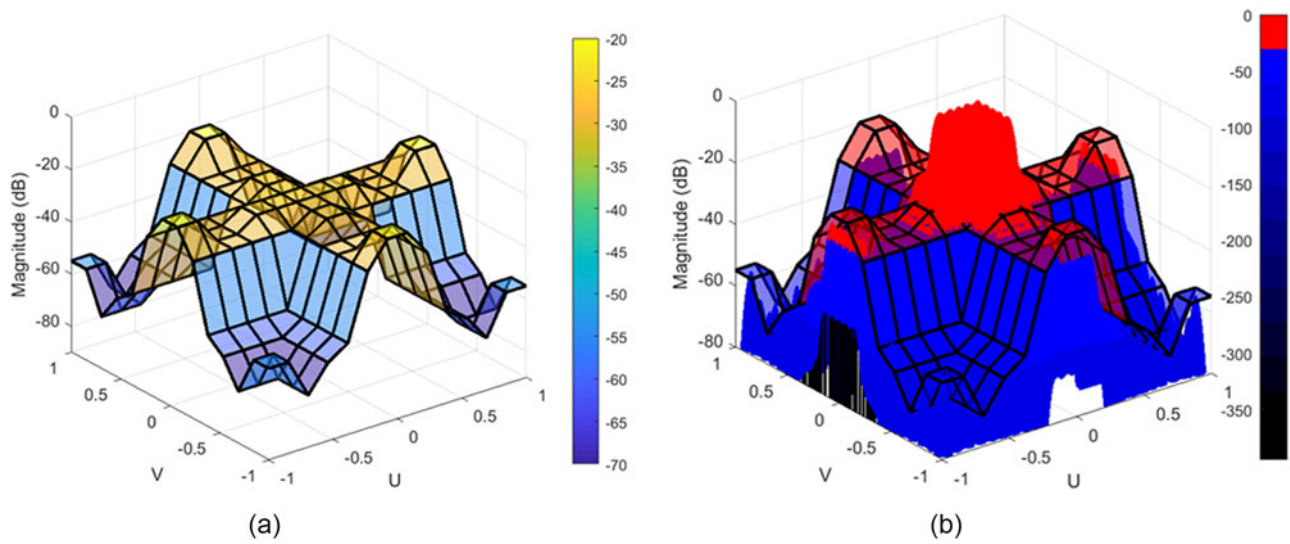


Figure 9. 3D coverage footprint pattern configuration: (a) a desired 3D mask grid template, (b) a desired 3D coverage footprint pattern.

the main beam has been preserved with the main beam steering in the required direction. In addition, the ability to fully control the levels of the sidelobes in other directions.

Test 3 (Linear array): for the third test, a scanned irregular amplitude-only linear array composed of $N = 20$ and 30, multi-beam steering is examined. Figures 3 and 4 show the construction of a radiation pattern with 4 ($N = 20$) and 5 ($N = 30$) beams, respectively, according to the proposed masks. Here, the objective function provides the possibility of generating a multi-beam pattern in different directions in coordination with the PSO algorithm and controlling the undirected lobes to counteract the interference signals.

Test 4 (Linear array): for the fourth test, an irregular amplitude-only linear array to implement a flat beam pattern is investigated. Figure 5 presents a single wide flat beam pattern with the assumed mask having the following constraints: The RBW is 0.37 rad (20 deg.) with a different SLL of $-20 \leq \text{SLL (dB)} \leq -70$. This figure shows that the resulting pattern is located between

the boundaries of the composite region with small ripples being generated.

Planar array pattern shaping (3D Pattern)

In this section, the different 3D beam patterns of a planar array by modifying amplitude-only distribution based on a designed different 3D mask covering are studied.

Test 1 (planar array): for the first test, an unscanned irregular amplitude-only planar array composed of $N \times M = 50 \times 50$, regularly elements space distance ($dx = dy = 0.5\lambda$) is examined. Figure 6 illustrates a set of 3D single-pencil beam electric fields at $(u, v) = (0, 0)$ with a corresponding 3D mask grid. In all cases, the 3D pencil beam has RBW equal to 0.14 rad (8 deg.) and SLL surface at range $-30 \leq \text{SLL (dB)} \leq -100$. It is observed through these figures that any 3D shaping can be generated by the objective function in coordination with the PSO algorithm.

Test 2 (planar array): for the second test, a scanned irregular amplitude-only four beams planar array composed of $N \times M = 30 \times 30$ is examined. Figure 7 illustrates a 3D four beams electric field at $(u, v) = (-0.5, -0.5)$, $(-0.5, 0.5)$, $(0.5, -0.5)$, and $(0.5, 0.5)$ with a corresponding 3D mask grid. In all beams, the RBW is equal to 0.26 rad (14.9 deg.) and SLL surface at range $-30 \leq \text{SLL (dB)} \leq -80$.

Test 3 (planar array): for the third test, a scanned irregular amplitude-only nine beams planar array composed of $N \times M = 30 \times 30$ is examined. Figure 8 illustrates a 3D nine beams electric field at $(u, v) = (-0.5, -0.5)$, $(0, -0.5)$, $(0.5, -0.5)$, $(-0.5, 0)$, $(0, 0)$, $(0.5, 0)$, $(-0.5, 0.5)$, $(0, 0.5)$, and $(0.5, 0.5)$ with a corresponding 3D mask grid. In all beams, the MBW is equal to 0.26 rad (14.9 deg.) and SLL surface at range $-40 \leq \text{SLL (dB)} \leq -90$.

Test 4 (planar array): for the fourth test, an irregular amplitude-only square footprint beam planar array composed of $N \times M = 50 \times 50$ is examined. Figure 9 illustrates a 3D footprint beam electric field at an area coverage range of $0.4 \text{ rad} \times 0.4 \text{ rad}$ and SLL surface at range $-20 \leq \text{SLL (dB)} \leq -80$ with a corresponding 3D mask grid. In all the proposed pattern mask (2D and 3D) shaping, it is observed that good patterns with suitable beam properties for modern applications are achieved.

Conclusion

This paper investigates the composition of different 2D and 3D beam pattern shapes of linear and planar arrays using the PSO algorithm. By correctly choosing the amplitude-only distribution to the array elements (with zero phase excitation), the desired beam shapes are produced. Different 2D and 3D masks were designed with specific RBW and different levels of sidelobes. Various beam pattern shapes represented by unscanned 2D single-pencil beam, scanned 2D pencil beam, 2D multi-beam scanning, 2D wide flat beam with little ripple, unscanned 3D single-pencil beam, 3D multi-beam scanning, and footprint (or contour) pattern have been completed. The simulation results displayed that the proposed plan provided an accurate performance to meet the requirements of modern applications in terms of efficiency, robustness, and ease of implementation in the algorithm. The proposed approach is suitable for the synthesis of large linear and planar arrays, as well as it can be applied to other types such as circular, cylindrical, spherical, etc.

Acknowledgements. The author is appreciative of Ninevah University for providing the research facilities necessary to finish this study.

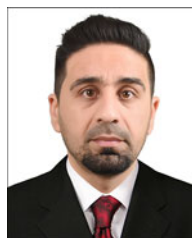
Funding statement. This research received no specific grant from any funding agency, commercial, or not-for-profit sectors.

Competing interests. The author report no conflict of interest.

References

- Rusek F, Persson D, Lau BK, Larsson EG, Marzetta TL, Edfors O and Tufvesson F (2013) Scaling up MIMO: Opportunities and challenges with very large arrays. *IEEE Signal Processing Magazine* **30**, 40–46.
- Mosalanejad M, Brebels S, Soens C, Ocket I and Vandenbosch GAE (2017) Millimeter wave cavity backed microstrip antenna array for 79 GHz radar applications. *Progress In Electromagnetics Research* **158**, 89–98.
- Morabito AF, Lagana AR and Di Donato L (2016) Satellite multibeam coverage of earth: Innovative solutions and optimal synthesis of aperture fields. *Progress In Electromagnetics Research* **156**, 135–144.
- Prasad S, Meenakshi M and Rao PH (2023) Three-dimensional shaped and contour pattern synthesis with multiple beam approach. *Microwave and Optical Technology Letters* **65**, 873–880.
- Prasad S, Meenakshi M and Rao PH (2023) Shaped beam from multiple beams using planar phased arrays. *Journal of Electromagnetic Waves and Applications* **37**, 592–604.
- Rudge A (1975) Multiple-beam antennas: Offset reflectors with offset feeds. *IEEE Transactions on Antennas and Propagation* **23**, 317–322.
- Butler J (1961) Beam-forming matrix simplifies design of electronically scanned antenna. *Electronic Design* **9**, 170–173.
- Ala-Laurinaho J, Aurinsalo J, Karttunen A, Kaunisto M, Lamminen A, Nurmiharju J, Räsänen AV, Säily J and Wainio P (2016) 2-D beam-steerable integrated lens antenna system for 5G E-band access and backhaul. *IEEE Transactions on Microwave Theory and Techniques* **64**, 2244–2255.
- Cherrette AR, Lee SW and Acosta RJ (1989) A method for producing a shaped contour radiation pattern using a single shaped reflector and a single feed. *IEEE Transactions on Antennas and Propagation* **37**, 698–706.
- Bhattacharyya AK (2007) Projection matrix method for shaped beam synthesis in phased arrays and reflectors. *IEEE Transactions on Antennas and Propagation* **55**, 675–683.
- Bornemann W, Balling P and English W (1985) Synthesis of spacecraft array antennas for intelsat frequency reuse multiple contoured beams. *IEEE Transactions on Antennas and Propagation* **33**, 1186–1193.
- Abdulqader AJ, Mohammed JR and Thaher RH (2020) Phase-only nulling with limited number of controllable elements. *Progress in Electromagnetics Research C* **99**, 167–178.
- Abdulqader AJ, Mahmood AN and Mohammed Ali YE (2022) A multi-objective array pattern optimization via thinning approach. *Progress in Electromagnetics Research C* **127**, 251–261.
- Orchard HJ, Elliott RS and Stern GJ (1985) Optimizing the synthesis of shaped beam antenna patterns. *IEE Proceedings Microwaves, Antennas, and Propagation* **132**, 63–68.
- Sánchez BJ, Covarrubias DH, Yepes LF, Panduro MA and Juárez E (2021) Effects of narrow beam phased antenna arrays over the radio channel metrics, Doppler power spectrum, and coherence time, in a context of 5G frequency bands. *Applied Sciences* **11**, e21.
- Quijano JLA, Righero M and Vecchi G (2014) Sparse 2-D array placement for arbitrary pattern mask and with excitation constraints: A simple deterministic approach. *IEEE Transactions on Antennas and Propagation* **62**, 1652–1662.
- Bucci OM, Isernia T, Morabito AF, Perna S and Pinchera D (2009) Aperiodic arrays for space applications: An effective strategy for the overall design. In *Proceedings of the 3rd European Conference on Antennas and Propagation, EuCAP 2009*, Berlin, Germany.
- Floudas CA and Pardalos PM (1996) *State of the Art in Global Optimization: Computational Methods and Applications*, IX. New York: Kluwer Academic Publishers.
- Abdulqader AJ, Mohammed JR and Ali YA (2022) A T-shaped polyomino subarray design method for controlling sidelobe level. *Progress in Electromagnetics Research C* **126**, 243–251.
- Mohammed JR, Thaher RH and Abdulqader AJ (2021) Linear and planar array pattern nulling via compressed sensing. *Journal of Telecommunications and Information Technology* **3**, 50–55.
- Zainud-Deen SH, Azzam DM and Malhat HAA (2020) 2D/3D shaped radiation patterns of sunflower and conformal antenna arrays using phase synthesis. *Wireless Personal Communications* **115**, 877–891.
- Albagory Y (2021) An efficient fast and convergence-controlled algorithm for Sidelobes Simultaneous Reduction (SSR) and spatial filtering. *Electronics* **10**, 1071.
- Salas-Sánchez AA, López-Álvarez C, Rodríguez-González JA, López-Martín ME and Ares-Pena FJ (2021) An improved pattern synthesis iterative method in planar arrays for obtaining efficient footprints with arbitrary boundaries. *Sensors* **21**, 2358.
- Kang M and Baek J (2022) Efficient and accurate synthesis for array pattern shaping. *Sensors* **22**, 5537.

25. **Abdulqader AJ, Mohammed JR and Thaher RH** (2020) Antenna pattern optimization via clustered arrays. *Progress in Electromagnetics Research M* **95**, 177–187.
26. **Ares-Pena FJ, Rodriguez-Gonzalez JA, Villanueva-Lopez E and Rengarajan SR** (1999) Genetic algorithms in the design and optimization of antenna array patterns. *IEEE Transactions on Antennas and Propagation* **47**, 506–510.
27. **Chen Y, Yang S and Nie Z** (2008) The application of a modified differential evolution strategy to some array pattern synthesis problems. *IEEE Transactions on Antennas and Propagation* **56**, 1919–1927.
28. **Woodward P** (1946) A method of calculating the field over a plane aperture required to produce a given polar diagram. *Journal of the Institution of Electrical Engineers-Part IIIA: Radiolocation* **93**, 1554–1558.
29. **Stutzman W** (1971) Synthesis of shaped-beam radiation patterns using the iterative sampling method. *IEEE Transactions on Antennas and Propagation* **19**, 36–41.
30. **Li JY, Qi YX and Zhou SG** (2017) Shaped beam synthesis based on superposition principle and Taylor method. *IEEE Transactions on Antennas and Propagation* **65**, 6157–6160.
31. **Prasad S, Meenakshi M, Adhithiya N, Rao PH, Krishna Ganti R and Bhaumik S** (2021) mmWave multibeam phased array antenna for 5G applications. *Journal of Electromagnetic Waves and Applications* **35**, 1802–1814.
32. **Storn R and Price K** (1997) Differential evolution—a simple and efficient heuristic for global optimization over continuous spaces. *Journal of Global Optimization* **11**, 341–359.
33. **Robinson J and Rahmat-Samii Y** (2004) Particle swarm optimization in electromagnetics. *IEEE Transactions on Antennas and Propagation* **52**, 397–407.
34. **Mohammed JR and Abdulqader AJ** (2022) Array pattern restoration under defective elements. *Progress in Electromagnetics Research C* **123**, 17–26.



Ahmed Jameel Abdulqader received the B.Sc. and M.Sc. degrees in Electronics and Communication Engineering from the University of Mosul, Iraq, in 2009 and 2013, respectively, and the Ph.D. degree in Communication Engineering from Mustansiriyah University, Iraq, in 2022. He is a lecturer at Ninevah University. His main research interests are in the area of the design and analysis of antenna arrays, array pattern optimization, mobile communication systems, and computer networks.